Centre for Computational Plasma Physics Annual Meeting

University of Warwick, November 9, 2015

Developments related to the radiation hydrodynamic code CHIC and ICF applications

V. T. Tikhonchuk, J. Breil

Centre Laser Intenses et Applications
University of Bordeaux, CNRS, CEA

Outline

1. **Missions of the group of high energy density physics in CELIA and available numerical tools**
2. **Major features of the CHIC code**
   - **Hydrodynamic model: ALE multi-material**
   - **Electron thermal transport: nonlocal effects**
   - **Fast electron transport: reduced kinetics**
   - **MHD package**
   - **Equations of state: low temperature limit**
   - **Radiative transport and opacities**
   - **Laser energy deposition: beyond ray tracing**
   - **Inline diagnostic tools**
3. **Future developments**

Missions of the plasma physics group

Plasma physics group in CELIA was created in 2003 for the academic support of the LMJ-PETAL facility constructed in the CEA/CESTA centre

Actually group involves:

- **3 academics**
- **2 permanents researchers CNRS**
- **10 permanents researchers CEA**
- **14 PhD students**
- **3 post doctoral fellows**

Missions of the group "Interaction, Inertial Confinement Fusion and Laboratory Astrophysics" are:

- **Development of the theoretical models and numerical tools for the high energy physics studies with high power lasers**
- **Support of dedicated experiments: design and interpretation**

Research subjects and numerical tools

Research subjects cover all domains of High Energy Density Physics:

- Inertial confinement fusion for energy
- New sources of energetic particles and radiation
- Laser-matter interaction
- Laboratory astrophysics
- Radiotherapy and laser processing

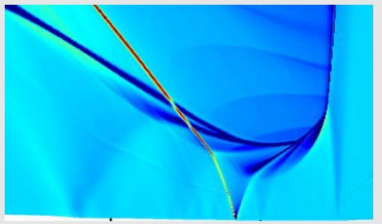

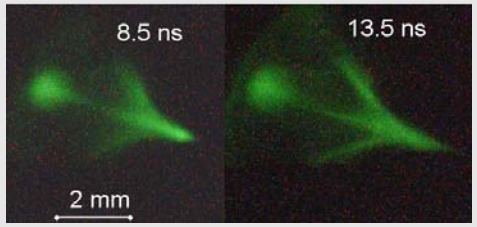

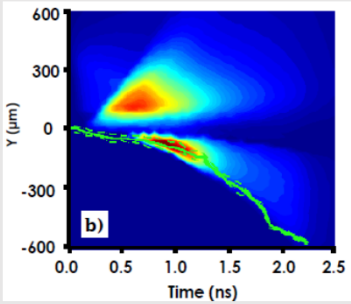

Numerical tools are designed in the group and in collaboration:

- Radiation hydrodynamic code CHIC
- Particle-in-Cell codes PICLS and OCEAN
- Fast kinetic codes M1 and M2 for the fast particle and radiation transport for HEDP and medical applications
- Paraxial electromagnetic code and full 3D Maxwell code for laser propagation in transparent dielectrics

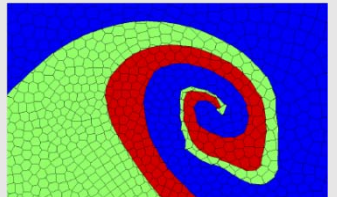

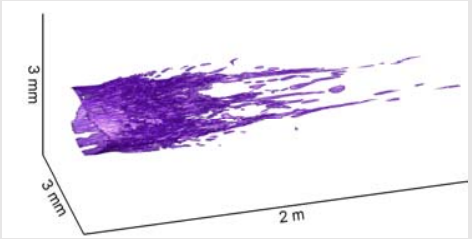

Radiation hydrodynamic code CHIC: structure

Code CHIC (Code of Hydrodynamic and Implosion of Celia) has been developed in 2003 – 2007, used for interpretation of experiments and ICF target designs

Managers: J. Breil, J.-L. Dubois

Developers: B. Chimier, G. Duchateau, J.-E. Ducret, J.-L. Feugeas, E. Le Bel, T. Nguen-Bui, Ph. Nicolai, X. Ribeyre, G. Schurtz

Collaborators:

- P.-H.Maire, L. Hallo, M. Olazabal-Loumé (CEA/CESTA)
- R. Liska, M. Kucharik, P. Vachal (Czech Univ. Prague)
- H. Nagamoto, A. Sunahara (Osaka Univ.)
- S. Glockner (I2M, Bordeaux Univ.)
- M. Shashkov (LANL, Los Alamos)
- M. Owen (LLNL, Livermore)
- A. Barlow (AWE)

Access: local usergroup

Remote access: exceptionally on demand

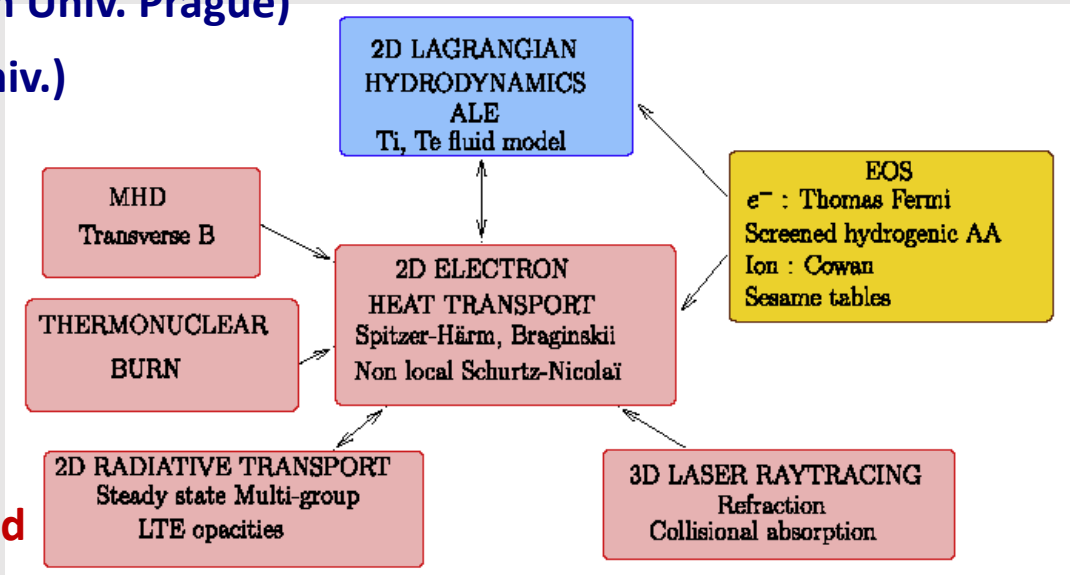

J. BREIL, S. GALERA, P.-H. MAIRE, *Multi-Material ALE computation in Inertial Confinement Fusion code CHIC*, Computers and Fluids, **46**, 161-167 (2011)

Radiation hydrodynamic code CHIC: features

Major features:

- **Arbitrary Lagrangian-Eulerian two-temperature hydrodynamics on a non-structured mesh, multi-material with remapping 2D-axisymmetric**
- **Electron and ion heat transport (Spitzer-Härm with flux limiter and Braginskii), nonlocal multi-group electron transport (model Schurtz, Nicolaï, Busquet)**
- **Reduced kinetic model for the fast charged particle transport (M1)**
- **A choice of equation-of-state models: SESAME, QEoS**
- **Laser energy deposition: 3D ray tracing and Bremsstrahlung absorption**
- **Generation of the azimuthal magnetic field according to the generalized Ohm's law**
- **Multi-group radiation transport: diffusion approximation with tabulated opacities**
- **Diffusion transport of α-particles**

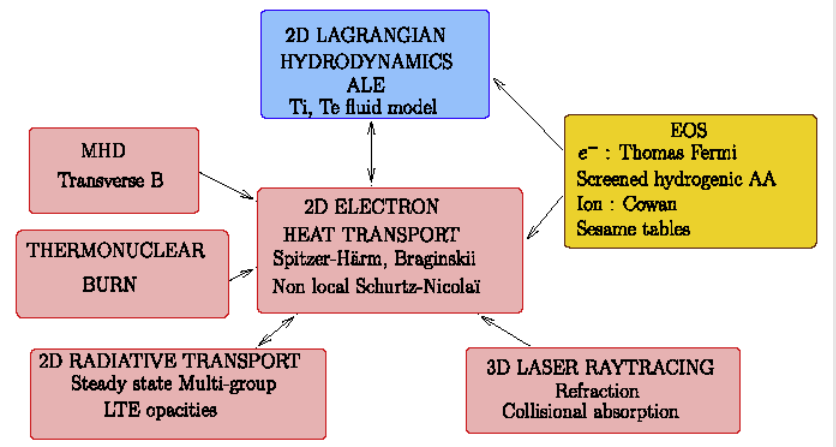

Hydrodynamic engine in the code CHIC

Major features:

- Unstructured cell-centered Lagrangian scheme
- Piecewise linear reconstruction
- Monotony ensured by slope limiters
- Extrapolated values of the velocity & pressure at the nodes
- Second order time discretization using RK2
- Conservative for momentum and total energy
- Compatible with GCL and entropy consistent

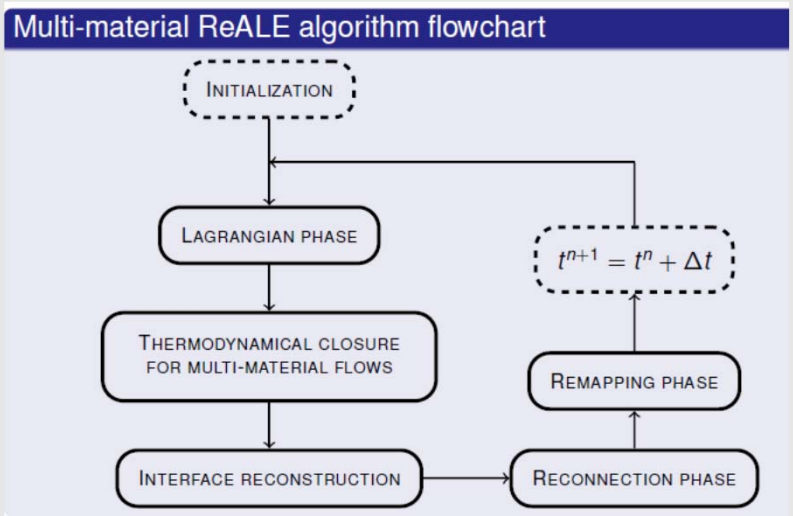

Multi-material treatment – Moment of Fluid (MOF):

- Based on Volume Fraction and Centroid tracking of each material
- Minimizes the discrepancy between the centroid of reconstructed polygon and the reference one
- No information from neighboring cells is needed, VOF
- Automatic (optimal) ordering of the materials
- Work for planar and axisymmetric geometry
- Second-order accurate
- Work on polygonal cell

Cell-centered quantities easier to handle in ALE and ReALE framework

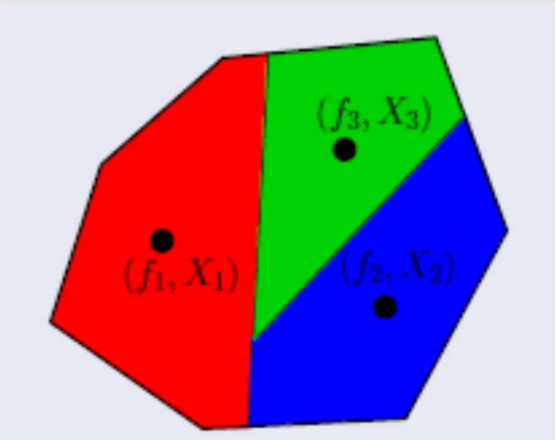

H.T. Ahn, M. Shashkov, JCP 2007; J. Breil et al, Computers & Fluids 2012

Reconnection and re-mapping technique

Grid relaxation:

- Convex combination of Lagrangian and rezoned meshes
- Minimizes the discrepancy between the centroid of reconstructed polygon and the reference one
- Prevents un-physical mesh motion
- No rezoning for uniform translation or rotation
- Galilean invariance

Reconnection-based rezoning:

- Voronoi tasselation
- Multi-material cell-intersection remapping
- Pure cell-swept-face remapping
- Hybrid: combination of swept flux and intersection remapping
- Conservative cell-centered interpolation
- High order piecewise monotonic linear reconstruction
- Cell shape may change after reconnection
- Combination with AMR methods

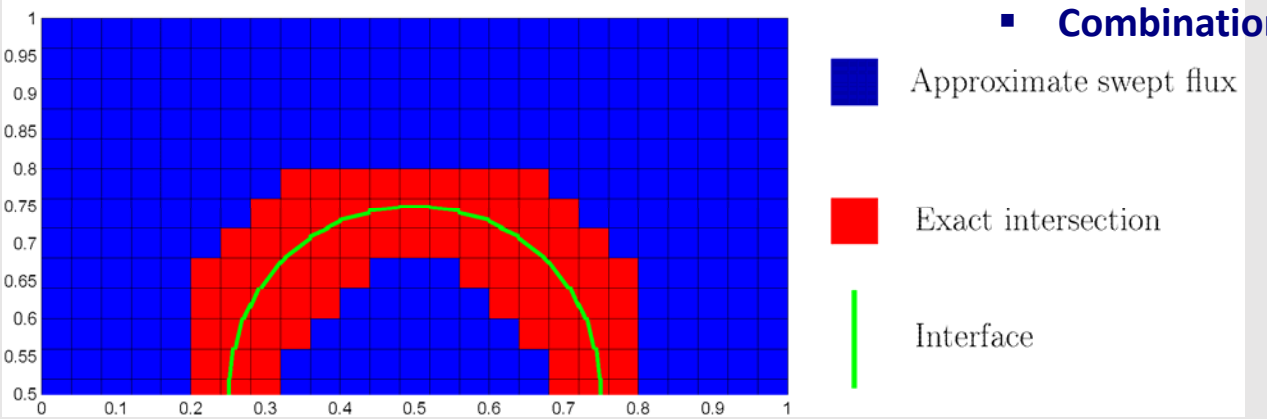

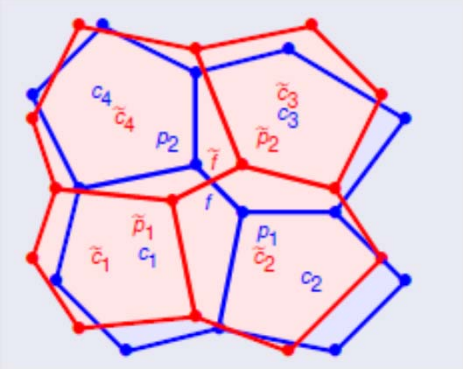

S. Galera et al, JCP 2010; R. Loubère et al, JCP 2010
T. Harribey et al, Int J Numer Meth Fluids 2013
M. Berndt et al, JCP 2011

Example of the hydro performance: Sedov explosion

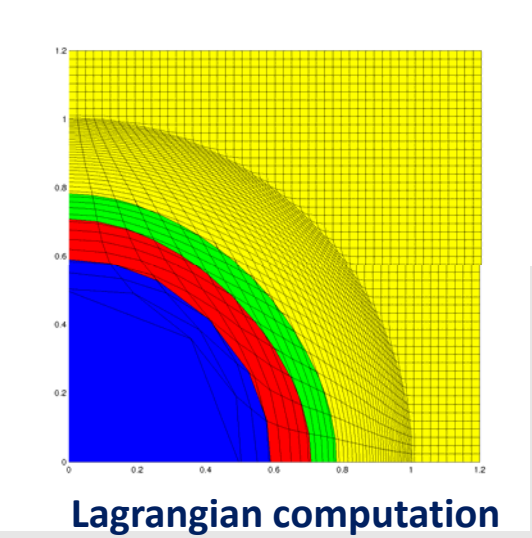

Lagrangian computation

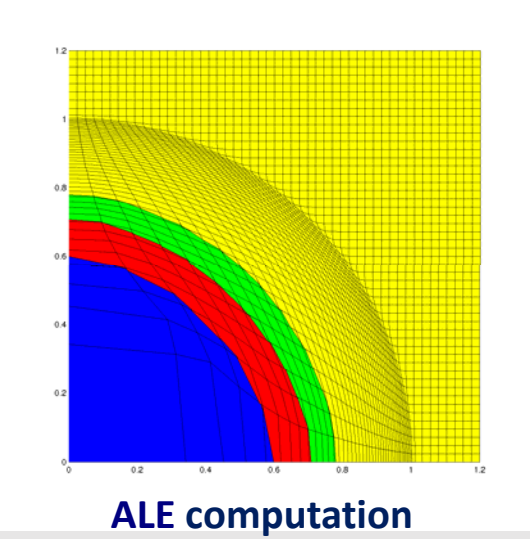

ALE computation

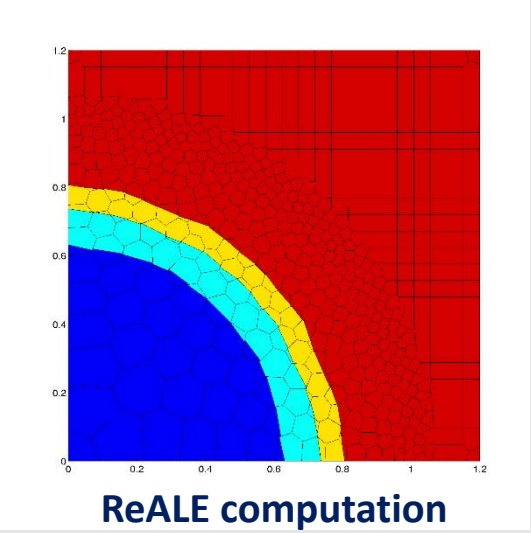

ReALE computation

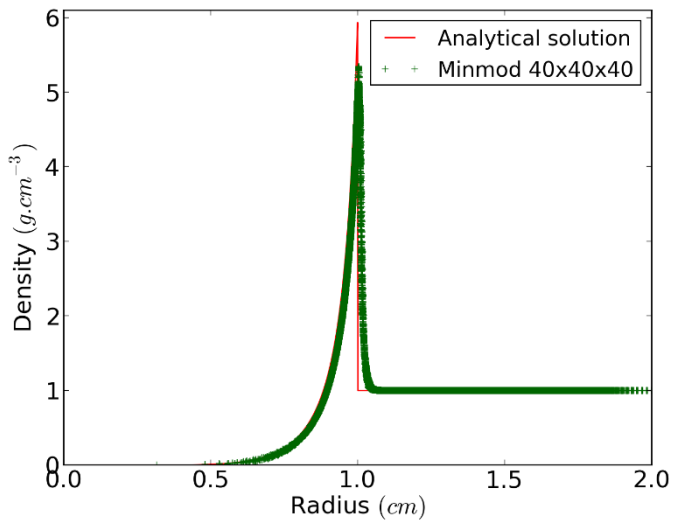

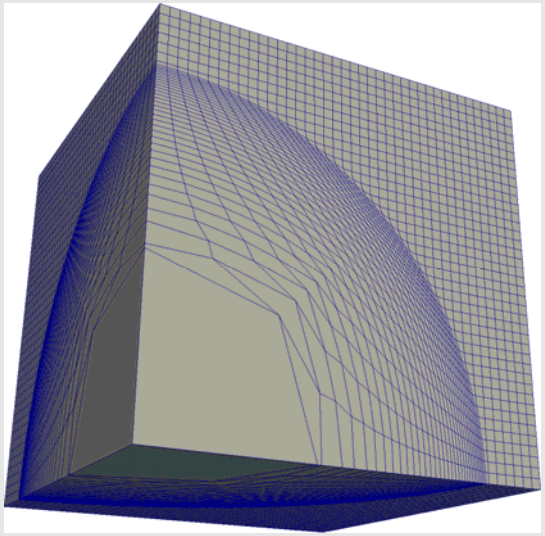

Electron energy transport: SNB scheme

Multi-group approach provides an efficient framework for the electron energy transport modeling in three dimensions and in the nonlocal regime

$$\mathbf{Q} = \mathbf{Q}_{SH} - \tfrac{1}{6} m_e \sqrt{Z} \int dp\, p^2 \mathrm{v}^3 \lambda_{\mathrm{corr}} \nabla \delta f_0$$

$$\mathbf{Q}_{SH} = -\kappa_{SH} \nabla T_e$$

$$\left(\lambda_{\mathrm{eff}}^{-1} - \tfrac{1}{3} \nabla \lambda_{\mathrm{corr}} \nabla\right) \delta f_0 = -g\, \mathrm{div}\, \mathbf{Q}_{SH}$$

$$g(p) \propto p^4 \exp\left(-p^2 / 2 m_e T_e\right)$$

$$\lambda_{\mathrm{eff}} = \mathrm{v} / \sqrt{\nu_{\mathrm{ee}} \nu_{\mathrm{ei}}} \qquad \lambda_{\mathrm{corr}}^{-1} = \lambda_{\mathrm{eff}}^{-1} + 2eE / p$$

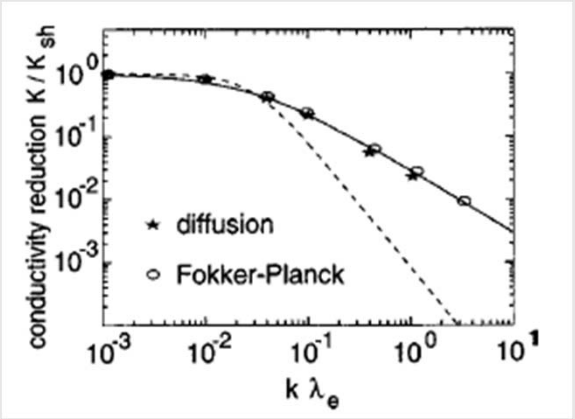

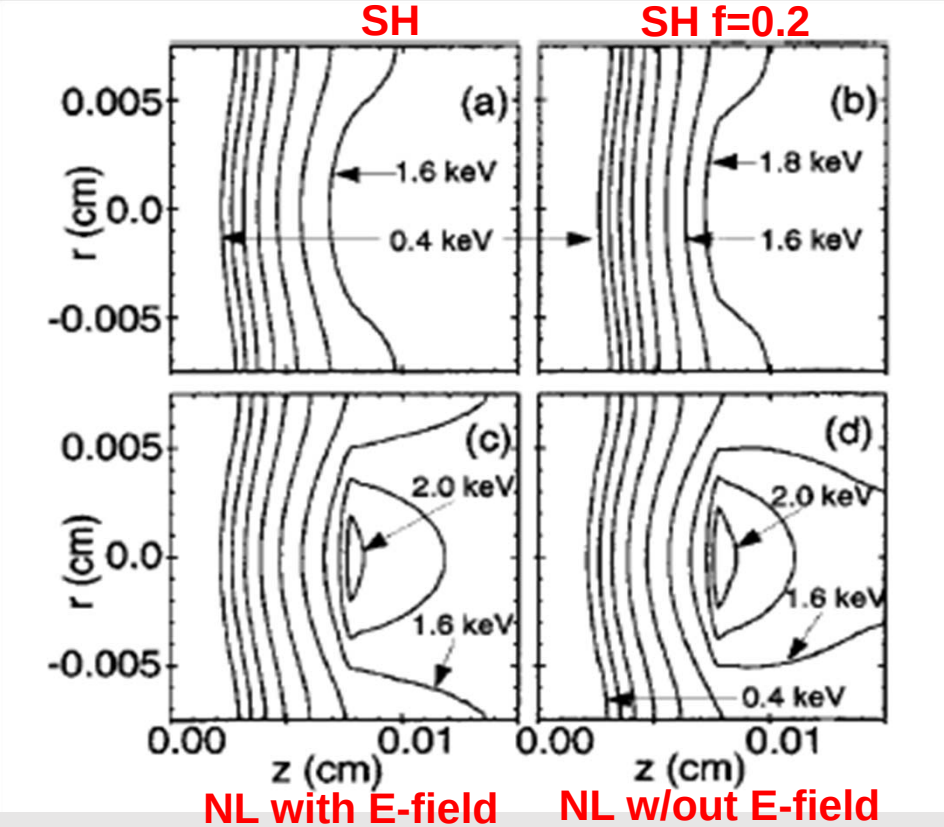

G. Schurtz et al, Phys Plasmas 2000
Ph. Nicolai et al, Phys Plasmas 2006

Magnetic field generation and nonlocal transport

Azimuthal magnetic field is calculated from the generalized Ohm's law

$$\partial_t \mathbf{B} = -\nabla \times \mathbf{E} = -\frac{1}{en_e}\nabla n_e \times \nabla T_e$$

$$\omega_{ce}\tau_e = eB / m_e \nu_{ei}$$

$$\mathbf{q}_e = -\kappa_\perp \nabla T_e - \kappa_\wedge \mathbf{b} \times \nabla T_e$$

Example of 2D energy transport

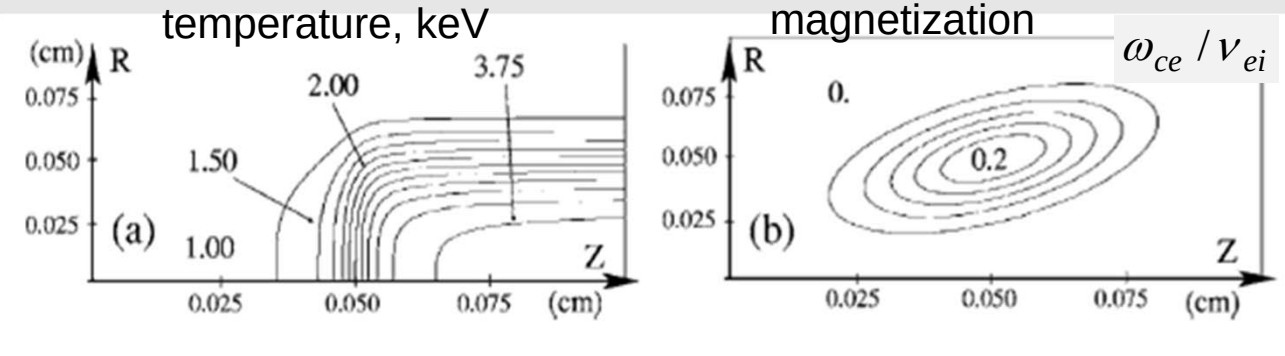

Temperature in keV

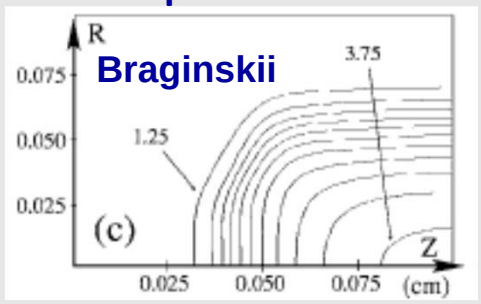

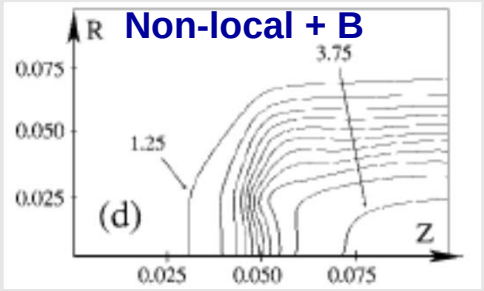

- **Suppression of the axial heat flux**
- **Strong axial preheat**
- **Weaker effect on the radial heat flux**
- **Steeper temperature profiles**

Reduced kinetic model of electron transport: M1

Reduced multi-group kinetic model M1 describes a directional electron transport

- **Closure for the second order term accounts for a strong anisotropy**
- **Positivity of the underlying distribution function**
- **Electron-electron collisions are accounted in the continuous slowing down approximation with angular scattering correction**

$$f_e^{\text{approx}}(\mathbf{p}) = g_e(p)\exp\left[\Omega\cdot\mathbf{a}_e(p)\right]$$

$$\mathbf{f}_{e2}(p) = \tfrac{1}{3}(1-\mu)f_{e0}\mathbf{I} + \mu\, f_{e0}\Omega_\varepsilon\otimes\Omega_\varepsilon$$

$$\Omega_\varepsilon = \mathbf{f}_{e1}/f_{e0}$$

$$\mu \cong \tfrac{1}{2}\Omega_\varepsilon^2\left(1+\Omega_\varepsilon^2\right)$$

Equations for the f_{e0} and f_{e1} follow from the FP equation

$$\mathrm{v}\nabla\cdot\mathbf{f}_{e1} - ep^{-2}\mathbf{E}\cdot\partial_p\left(p^2\mathbf{f}_{e1}\right) = p^{-2}\partial_p\left(p^2 S_M f_{e0}\right)$$

$$\tfrac{1}{3}\mathrm{v}\nabla\cdot\mathbf{f}_{e2} - ep^{-2}\mathbf{E}\cdot\partial_p\left(p^2\mathbf{f}_{e2}\right) = p^{-2}\partial_p\left(p^2 S_M\mathbf{f}_{e1}\right) - \nu_{ei}\mathbf{f}_{e1} - ep^{-1}\left(\mathbf{E}f_{e0} - \mathbf{E}\cdot\mathbf{f}_{e2} + \mathrm{v}\mathbf{f}_{e1}\times\mathbf{B}\right)$$

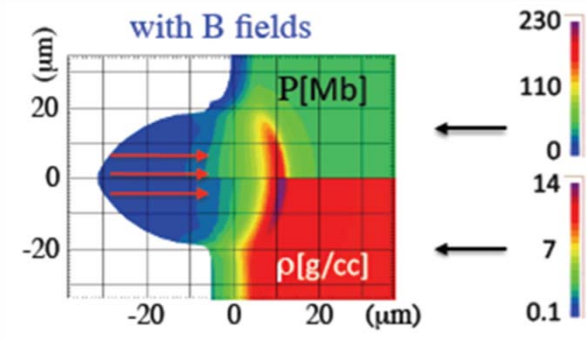

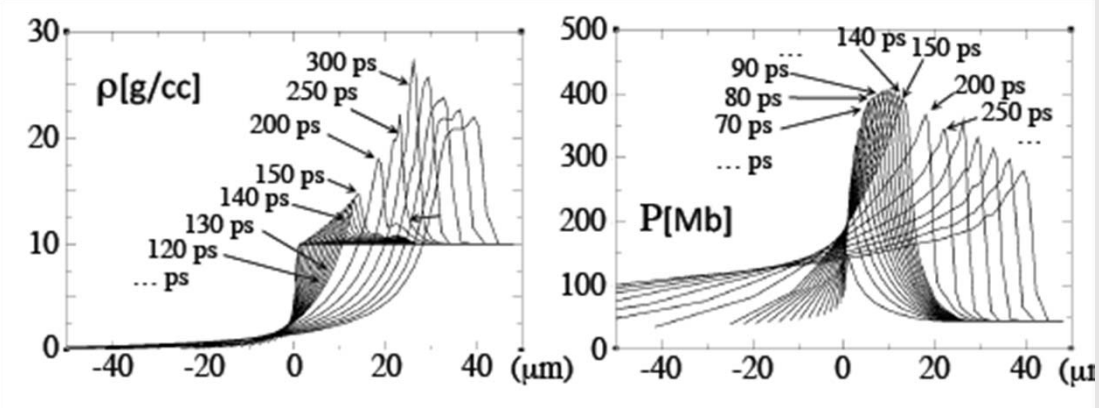

Ph. Nicolai et al, Phys. Rev. E 2011, 2014
M. Touati et al. NJP 2014

Advanced laser energy deposition model: thick rays

New approach of paraxial complex geometrical optics describes the laser intensity in corona and takes into account: speckled intensity distribution, the cross beam energy transfer, ponderomotive force, excitation of parametric instabilities and hot electrons

$$E_{\text{las}}(\vec{r}) = A(\vec{r})\, e^{i\varphi(\vec{r})}$$

$$\varphi(\vec{r}) = \varphi(r_{\parallel}) + \frac{1}{2} B_{ij} r_{\perp i} r_{\perp j}$$

Ray centroid Ray curvature/width

Central ray equation

$$d\vec{r}/d\tau = \vec{v}$$

$$d\vec{v}/d\tau = {}^{1}/_{2}\, \nabla\epsilon(\vec{r})$$

$$dP/d\tau = -\kappa P$$

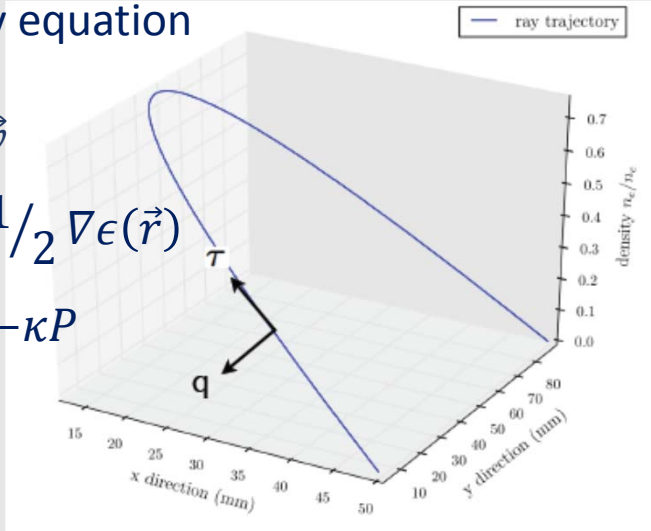

Beam width $w(\tau) = \sqrt{2/k_0 \mathrm{Im} B(\tau)}$

Beam curvature $\rho(\tau) = \sqrt{\epsilon_c'}/\mathrm{Re} B(\tau)$

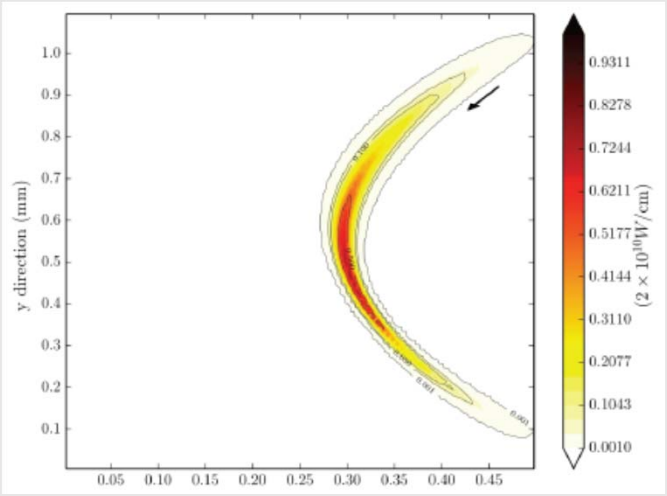

Wave front equation in the ray reference frame

$$B^2 + \frac{dB}{d\tau} = -\frac{3}{4\epsilon}\left(\frac{d\epsilon}{dq}\right)^2 + \frac{1}{2}\frac{d^2\epsilon}{dq^2}$$

Y A Kravtsov, N A Zhu, *Theory of Diffraction*, Oxford 2010

A Colaitis et al, PRE 2014

Cross-beam energy transfer (CBET) with thick rays

CBET is validated by comparison with the paraxial electromagnetic code HARMONY

Test case – expanding foil

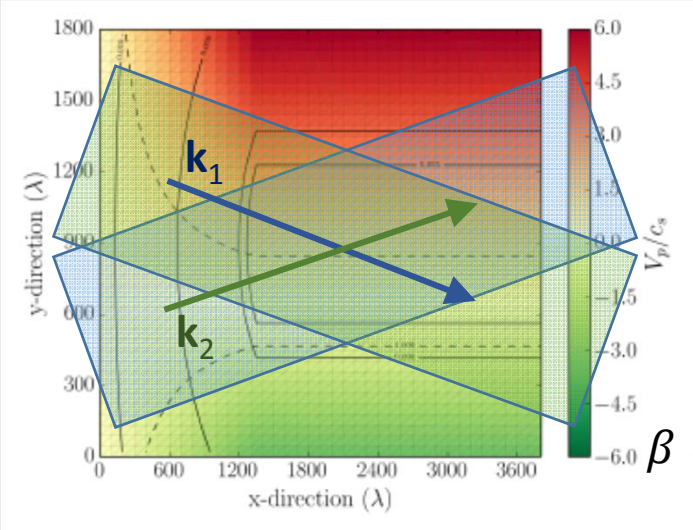

$$\partial_\xi I_1 = -2\beta I_1 I_2$$

$$\partial_\eta I_2 = 2\beta I_1 I_2$$

$$\beta = \frac{\omega_e^2 \omega_s^2 \nu_s \omega}{\omega_2 \nu_2 \left[\left(\omega_s^2 - \omega^2 \right)^2 + 4\omega_s^2 \omega^2 \right]}$$

Probe amplification

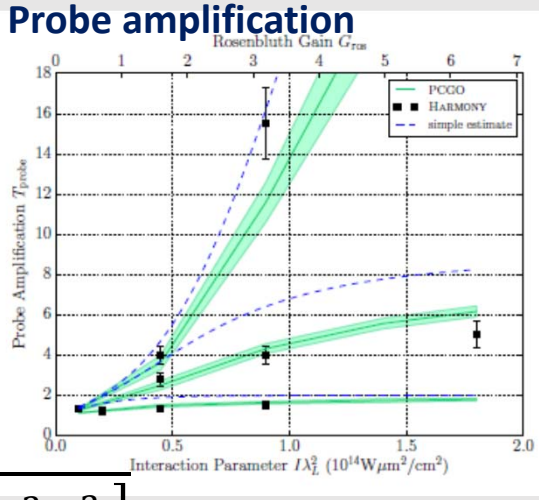

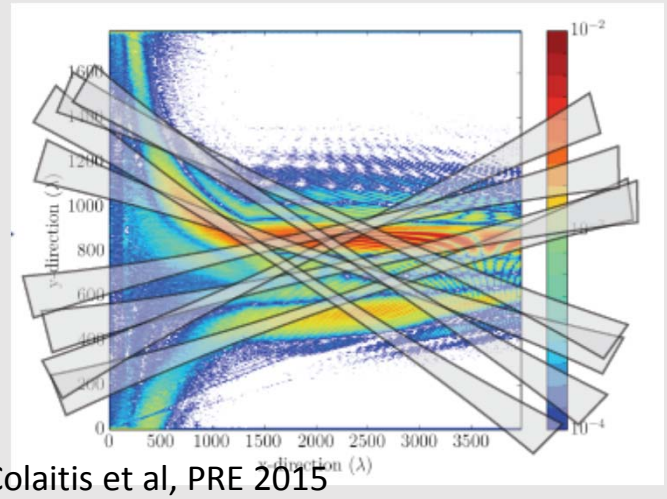

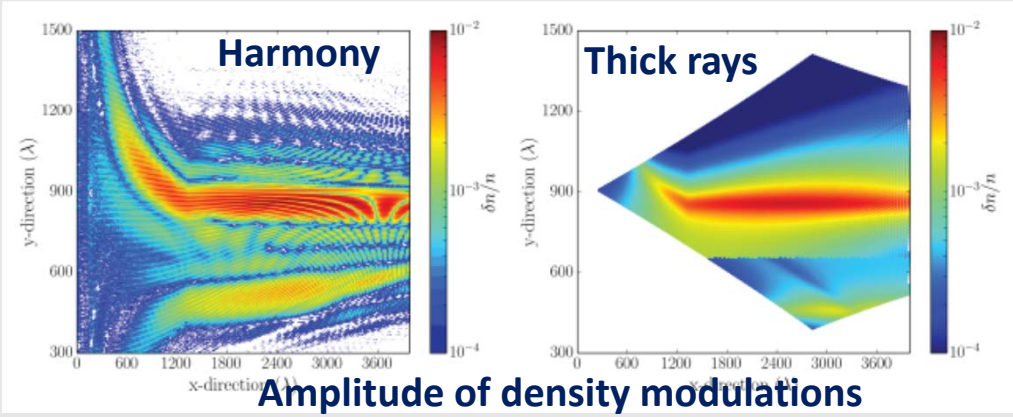

Amplitude of density modulations

A Colaitis et al, PRE 2015

S. Hüller et al, IFSA 2015

Thick ray model of laser plasma interaction

The model describes the collisional absorption and the hot electron generation due to the resonance absorption, SRS and TPD of each laser beamlet

Resonance absorption

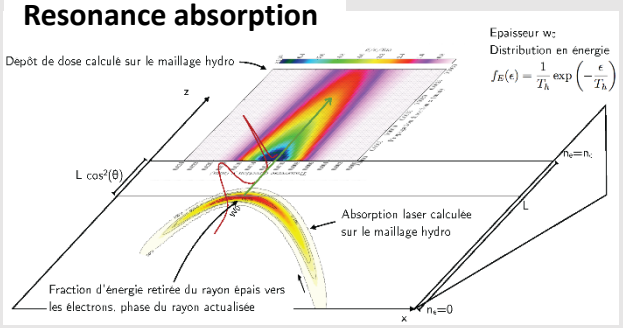

Stimulated Raman Scattering

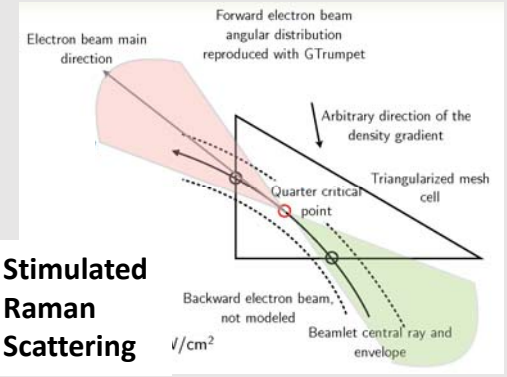

Two Plasmon Decay

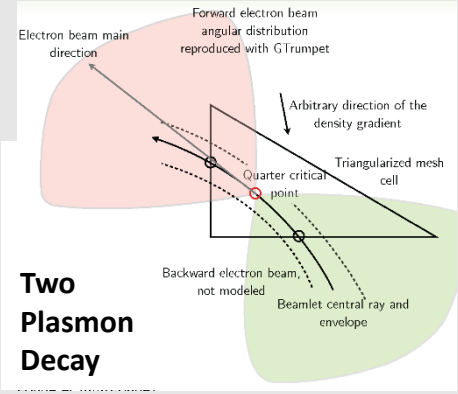

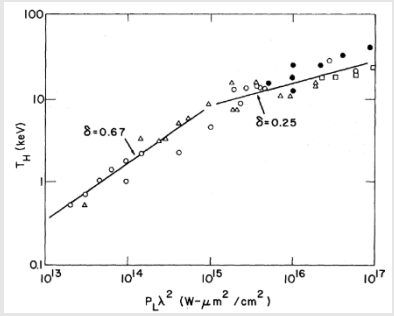

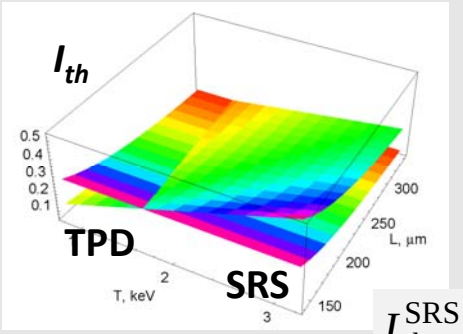

$$T_h^{\mathrm{SRS}} = \frac{1}{2} m_e v_{ph}^2$$

$$f_h(\varepsilon) \propto \exp -\frac{\varepsilon}{T_h}$$

$$T_h^{\mathrm{TPD}} = 15.5 + 17.7 I / I_{th} \ \mathrm{keV}$$

$$\eta_h = 0.026\left[1 - \exp\left(-\sqrt{I / I_{th} - 1}\right)\right]$$

$$I_{th}^{\mathrm{TPD}} = 8.2 T_{\mathrm{keV}} / L_{n\mu\mathrm{m}} \lambda_{\mu\mathrm{m}} \ \mathrm{PW/cm^2}$$

$$I_{th}^{\mathrm{SRS}} = 99.5 L_{n\mu\mathrm{m}}^{-4/3} \lambda_{\mu\mathrm{m}}^{-2/3} \ \mathrm{PW/cm^2}$$

D.W. Forslund et al, PRA 1974, PRL 1977

O Klimo et al, PPCF 2013, 2014

R Yan et al, PRL 2012
HX Vu et al, Phys Plasmas 2012

Propagation of hot electron Gaussian beamlets is described in the Continuous Slowing Down approximation including angular scattering

A Colaitis et al, PRE 2015

Strong shock driven by hot electrons (PALS experiment)

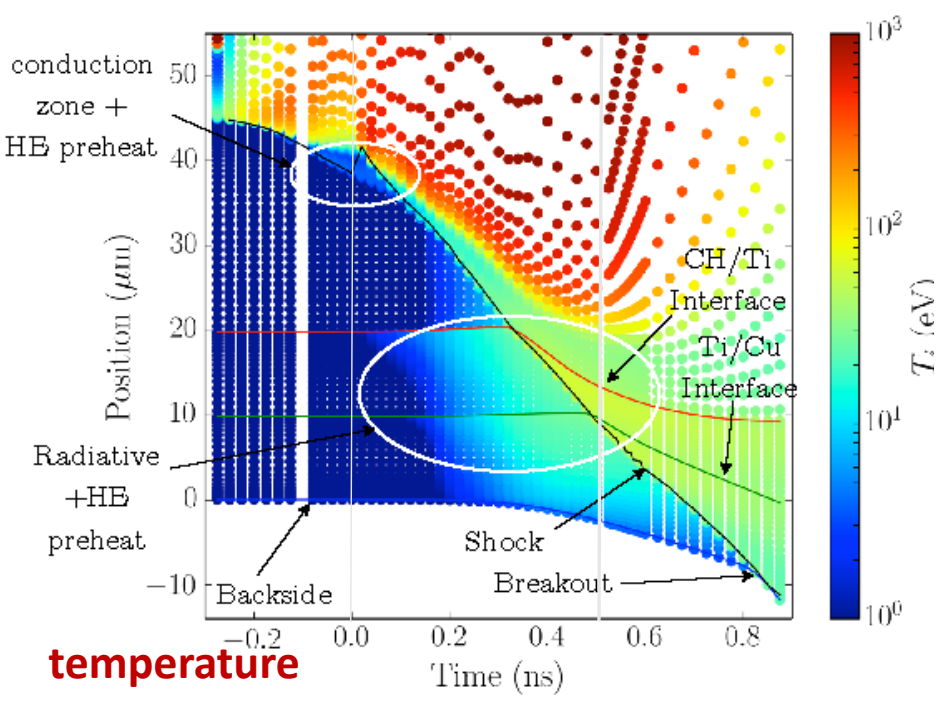

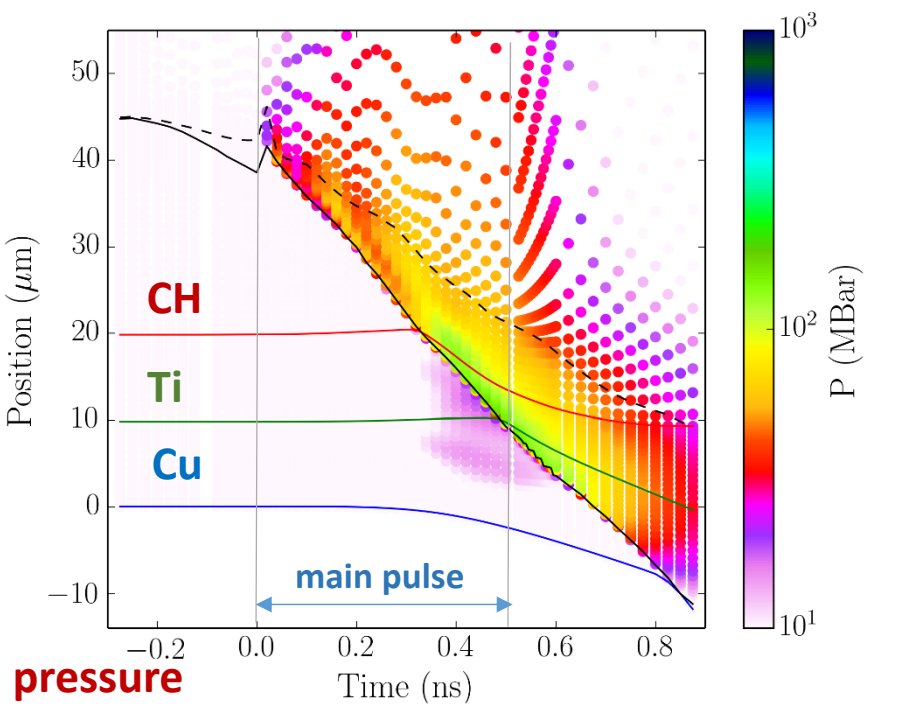

- **Hot electron generation is due to the SRS and TPD**
- **Hot electrons increase the shock pressure by less than 30% and accelerate the shock**
- **Hot electrons preheat upstream target to > 10 eV and reduce shock strength by a factor of 10-20**
- **Hot electron preheat initiates the target expansion thus delaying the shock breakout**

D Batani et al, Phys Plasmas 2014
A Colaitis et al, PRE 2015

Plasma diagnostics: X-rays

X-ray diagnostics provide an information about the plasma density and temperature distributions in a direct comparison with experimental results: imaging, radiography, spectroscopy

X-ray Imaging

$$I_\nu(s) = \frac{\varepsilon_\nu}{4\pi\kappa_\nu} + \left(I_\nu(0) - \frac{\varepsilon_\nu}{4\pi\kappa_\nu}\right) e^{-\kappa_\nu s}$$

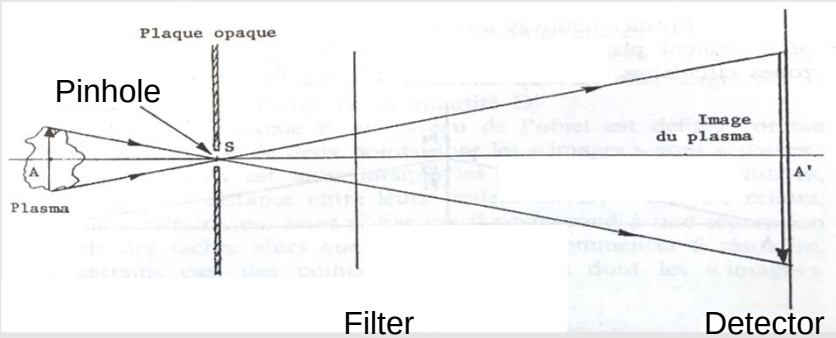

Spectroscopy

$$\mu \frac{\partial I_\nu}{\partial x} = j_\nu - \kappa_\nu I_\nu - \frac{8\pi}{3}\sigma_T I_\nu + \sigma_T \int d\mu' \,(1 + (\mu\mu')^2) I'_\nu$$

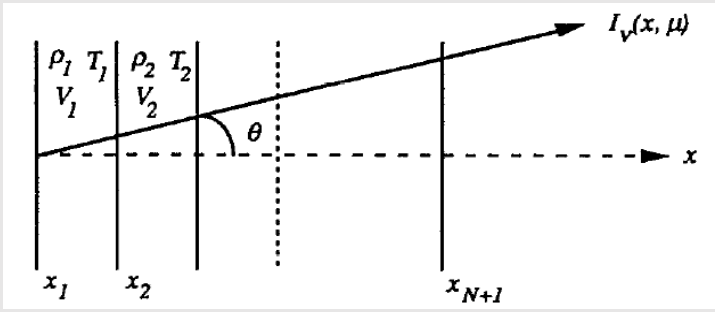

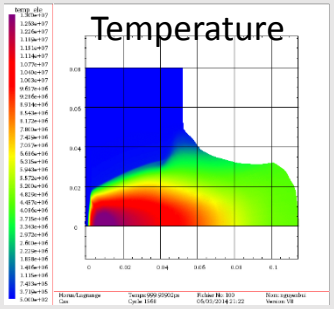

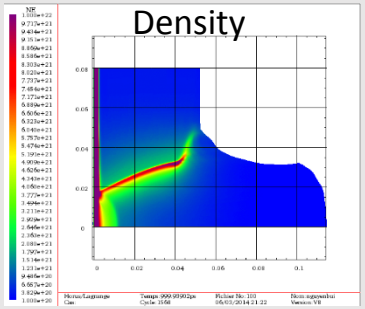

Simulation CHIC

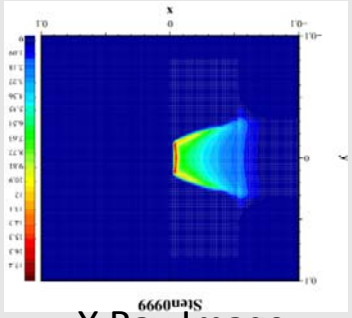

X Ray Image on Detector

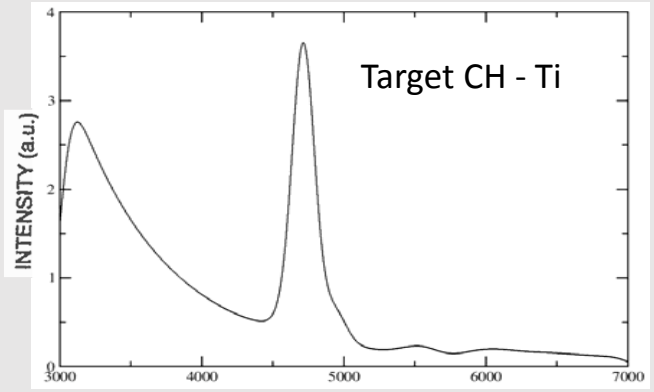

Plasma diagnostics: neutrons

Neutron diagnostics makes a link between the observed particle characteristics and the hydrodynamic parameters $\langle \rho R \rangle, \langle \rho \rangle, \langle T \rangle$

- **Neutron interaction in the target: elastic scattering on plasma nuclei, discrete process, probability ≤ a few %**
- **Neutron transport: a series of straight lines, with at most two elastic interactions**
- **Neutron production: integration of the fusion rates over columns crossing CHIC mesh**
- **Neutron imaging: annular & penumbral imaging included**

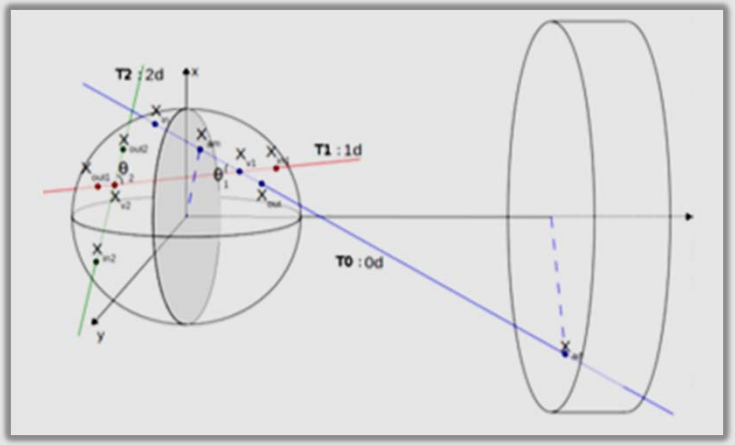

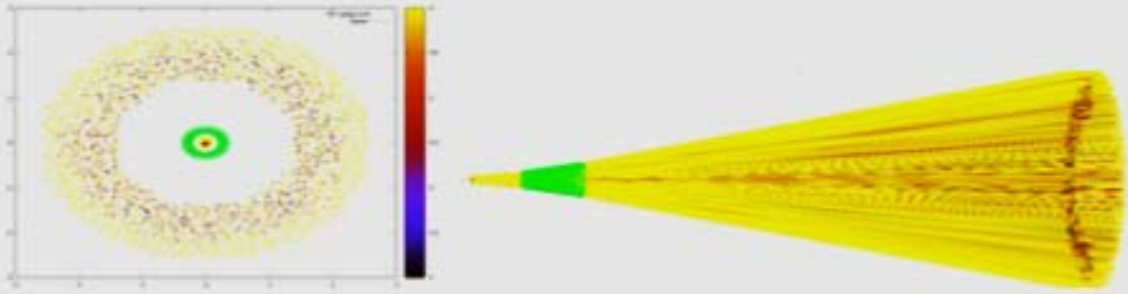

Conclusions – perspectives

CHIC includes several physical modules that are validated by comparison with many experiments. The code is used for theoretical studies, target design and interpretation of experiments.

Future developments within and/or beyond CHIC include:

- **Three-component magnetic field generation**
- **Kinetic transport of α-particles**
- **Validation of laser energy deposition with thick optical rays, CBET**
- **Improved nonlocal multi-group electron transport coupled to parametric instabilities**
- **Parallelization of time-consuming modules**
- **Improved interface and visualization tools**
- **Elasto-plastic model for the equation-of-state module**
- **Three dimensional hydrodynamics and diffusion modules**
- **Increase of the user's pool**

Developments of new physical modules and validation in experiments require extended collaborations